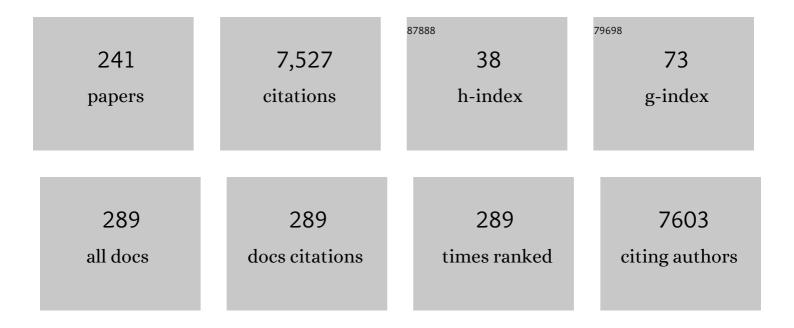
Marcus Christl

List of Publications by Year in descending order

Source: https://exaly.com/author-pdf/3895069/publications.pdf Version: 2024-02-01



#	Article	IF	CITATIONS
1	9,400 years of cosmic radiation and solar activity from ice cores and tree rings. Proceedings of the National Academy of Sciences of the United States of America, 2012, 109, 5967-5971.	7.1	557
2	Ancient Biomolecules from Deep Ice Cores Reveal a Forested Southern Greenland. Science, 2007, 317, 111-114.	12.6	393
3	Latest Pleistocene and Holocene glacier variations in the European Alps. Quaternary Science Reviews, 2009, 28, 2137-2149.	3.0	378
4	The GEOTRACES Intermediate Data Product 2017. Chemical Geology, 2018, 493, 210-223.	3.3	257
5	The ETH Zurich AMS facilities: Performance parameters and reference materials. Nuclear Instruments & Methods in Physics Research B, 2013, 294, 29-38.	1.4	252
6	Possible solar origin of the 1,470-year glacial climate cycle demonstrated in a coupled model. Nature, 2005, 438, 208-211.	27.8	231
7	Bats: A new tool for AMS data reduction. Nuclear Instruments & Methods in Physics Research B, 2010, 268, 976-979.	1.4	201
8	A 600â€year annual ¹⁰ Be record from the NGRIP ice core, Greenland. Geophysical Research Letters, 2009, 36, .	4.0	157
9	10Be and 26Al measurements at the Zurich 6MV Tandem AMS facility. Nuclear Instruments & Methods in Physics Research B, 2010, 268, 880-883.	1.4	144
10	Does sedimentary ²³¹ Pa/ ²³⁰ Th from the Bermuda Rise monitor past Atlantic Meridional Overturning Circulation?. Geophysical Research Letters, 2009, 36, .	4.0	119
11	Tree rings reveal globally coherent signature of cosmogenic radiocarbon events in 774 and 993 CE. Nature Communications, 2018, 9, 3605.	12.8	98
12	Eleven-year solar cycles over the last millennium revealed by radiocarbon in tree rings. Nature Geoscience, 2021, 14, 10-15.	12.9	97
13	Trench-Parallel Anisotropy Produced by Foundering of Arc Lower Crust. Science, 2007, 317, 108-111.	12.6	92
14	Deep water provenance and dynamics of the (de)glacial Atlantic meridional overturning circulation. Earth and Planetary Science Letters, 2016, 445, 68-78.	4.4	88
15	Dating the onset of LGM ice surface lowering in the High Alps. Quaternary Science Reviews, 2016, 143, 37-50.	3.0	87
16	Rapid increase in cosmogenic 14C in AD 775 measured in New Zealand kauri trees indicates short-lived increase in 14C production spanning both hemispheres. Earth and Planetary Science Letters, 2015, 411, 290-297.	4.4	86
17	The dependence of meteoric 10Be concentrations on particle size in Amazon River bed sediment and the extraction of reactive 10Be/9Be ratios. Chemical Geology, 2012, 318-319, 126-138.	3.3	71
18	Rapid Holocene thinning of an East Antarctic outlet glacier driven by marine ice sheet instability. Nature Communications, 2015, 6, 8910.	12.8	70

#	Article	IF	CITATIONS
19	The AD 1717 rock avalanche deposits in the upper Ferret Valley (Italy): a dating approach with cosmogenic ¹⁰ Be. Journal of Quaternary Science, 2012, 27, 383-392.	2.1	69
20	Spatial variability of 10 Be-derived erosion rates across the southern Peninsular Indian escarpment: A key to landscape evolution across passive margins. Earth and Planetary Science Letters, 2015, 425, 154-167.	4.4	67
21	First 236U data from the Arctic Ocean and use of 236U/238U and 129I/236U as a new dual tracer. Earth and Planetary Science Letters, 2016, 440, 127-134.	4.4	66
22	A first transect of 236U in the North Atlantic Ocean. Geochimica Et Cosmochimica Acta, 2014, 133, 34-46.	3.9	65
23	Plutonium release from Fukushima Daiichi fosters the need for more detailed investigations. Scientific Reports, 2013, 3, 2988.	3.3	64
24	The importance of independent chronology in integrating records of past climate change for the 60–8Âka INTIMATE time interval. Quaternary Science Reviews, 2014, 106, 47-66.	3.0	64
25	Competitive 10Be measurements below 1MeV with the upgraded ETH–TANDY AMS facility. Nuclear Instruments & Methods in Physics Research B, 2010, 268, 2801-2807.	1.4	63
26	Multiradionuclide evidence for an extreme solar proton event around 2,610 B.P. (â^1⁄4660 BC). Proceedings of the United States of America, 2019, 116, 5961-5966.	7.1	63
27	Post-Accident Sporadic Releases of Airborne Radionuclides from the Fukushima Daiichi Nuclear Power Plant Site. Environmental Science & Technology, 2015, 49, 14028-14035.	10.0	61
28	Status of 236U analyses at ETH Zurich and the distribution of 236U and 129I in the North Sea in 2009. Nuclear Instruments & Methods in Physics Research B, 2015, 361, 510-516.	1.4	58
29	The potential of He stripping in heavy ion AMS. Nuclear Instruments & Methods in Physics Research B, 2013, 294, 382-386.	1.4	57
30	An improved experimental determination of cosmogenic 10Be/21Ne and 26Al/21Ne production ratios in quartz. Earth and Planetary Science Letters, 2009, 284, 187-198.	4.4	56
31	A depth profile of uranium-236 in the Atlantic Ocean. Geochimica Et Cosmochimica Acta, 2012, 77, 98-107.	3.9	55
32	Reconstruction of the ²³⁶ <scp>U</scp> input function for the <scp>N</scp> ortheast <scp>A</scp> tlantic <scp>O</scp> cean: Implications for ¹²⁹ <scp>I</scp> / ²³⁶ <scp>U</scp> and ²³⁶ <scp>U</scp> and ²³⁶ <scp>U</scp> and ²³⁶ <scp>U</scp> and	2.6	46
33	Research: Oceans, 2015, 120, 7282-7299. Copperâ€nickelâ€rich, amalgamated ferromanganese crustâ€nodule deposits from Shatsky Rise, NW Pacific. Geochemistry, Geophysics, Geosystems, 2012, 13, .	2.5	44
34	Beryllium-10 in deep-sea sediments: a tracer for the Earth's magnetic field intensity during the last 200,000 years. Quaternary Science Reviews, 2003, 22, 725-739.	3.0	43
35	Evidence for a link between the flux of galactic cosmic rays and Earth's climate during the past 200,000 years. Journal of Atmospheric and Solar-Terrestrial Physics, 2004, 66, 313-322.	1.6	43
36	Multiple cosmogenic nuclides document complex Pleistocene exposure history of glacial drifts in Terra Nova Bay (northern Victoria Land, Antarctica). Quaternary Research, 2009, 71, 83-92.	1.7	42

#	Article	IF	CITATIONS
37	A test of the cosmogenic ¹⁰ Be(meteoric)/ ⁹ Be proxy for simultaneously determining basin-wide erosion rates, denudation rates, and the degree of weathering in the Amazon basin. Journal of Geophysical Research F: Earth Surface, 2015, 120, 2498-2528.	2.8	41
38	A deglaciation model of the Oberhasli, Switzerland. Journal of Quaternary Science, 2016, 31, 46-59.	2.1	41
39	Marine radioecology after the Fukushima Dai-ichi nuclear accident: Are we better positioned to understand the impact of radionuclides in marine ecosystems?. Science of the Total Environment, 2018, 618, 80-92.	8.0	39
40	Tracing the Three Atlantic Branches Entering the Arctic Ocean With ¹²⁹ I and ²³⁶ U. Journal of Geophysical Research: Oceans, 2018, 123, 6909-6921.	2.6	38
41	First data of Uranium-236 in the North Sea. Nuclear Instruments & Methods in Physics Research B, 2013, 294, 530-536.	1.4	36
42	Isochronâ€burial dating of glaciofluvial deposits: First results from the Swiss Alps. Earth Surface Processes and Landforms, 2017, 42, 2414-2425.	2.5	36
43	10Be AMS measurements at low energies (E<1MeV). Nuclear Instruments & Methods in Physics Research B, 2008, 266, 2207-2212.	1.4	35
44	Evidence of central Alpine glacier advances during the Younger Dryas–early Holocene transition period. Boreas, 2016, 45, 398-410.	2.4	35
45	Regional mid-Pleistocene glaciation in central Patagonia. Quaternary Science Reviews, 2017, 164, 77-94.	3.0	35
46	Potential Releases of ¹²⁹ I, ²³⁶ U, and Pu Isotopes from the Fukushima Dai-ichi Nuclear Power Plants to the Ocean from 2013 to 2015. Environmental Science & Technology, 2017, 51, 9826-9835.	10.0	35
47	¹⁰ Be systematics in the Tsangpo-Brahmaputra catchment: the cosmogenic nuclide legacy of the eastern Himalayan syntaxis. Earth Surface Dynamics, 2017, 5, 429-449.	2.4	35
48	Ultra-trace determination of plutonium in urine samples using a compact accelerator mass spectrometry system operating at 300 kV. Journal of Analytical Atomic Spectrometry, 2012, 27, 126-130.	3.0	34
49	Isotopic signature of plutonium at Bikini atoll. Applied Radiation and Isotopes, 2010, 68, 979-983.	1.5	33
50	Timing of European fluvial terrace formation and incision rates constrained by cosmogenic nuclide dating. Earth and Planetary Science Letters, 2016, 451, 221-231.	4.4	33
51	Radionuclide pollution inside the Fukushima Daiichi exclusion zone, part 2: Forensic search for the "Forgotten―contaminants Uranium-236 and plutonium. Applied Geochemistry, 2017, 85, 194-200.	3.0	33
52	Denudation variability of the <scp>S</scp> ila <scp>M</scp> assif upland (<scp>I</scp> taly) from decades to millennia using <scp>¹⁰Be</scp> and ²³⁹⁺²⁴⁰ <scp>Pu</scp> . Land Degradation and Development, 2018, 29, 3736-3752.	3.9	33
53	New geomorphological and chronological constraints for glacial deposits in the Rivoliâ€Avigliana endâ€moraine system and the lower Susa Valley (Western Alps, NW Italy). Journal of Quaternary Science, 2018, 33, 550-562.	2.1	32
54	Late-Pleistocene catchment-wide denudation patterns across the European Alps. Earth-Science Reviews, 2020, 211, 103407.	9.1	32

#	Article	IF	CITATIONS
55	Reduced sediment supply in a fast eroding landscape? A multi-proxy sediment budget of the upper Rhône basin, Central Alps. Sedimentary Geology, 2018, 375, 105-119.	2.1	31
56	Catchment-wide weathering and erosion rates of mafic, ultramafic, and granitic rock from cosmogenic meteoric 10Be/9Be ratios. Geochimica Et Cosmochimica Acta, 2018, 222, 618-641.	3.9	31
57	Reconstruction of global 10Be production over the past 250ka from highly accumulating Atlantic drift sediments. Quaternary Science Reviews, 2010, 29, 2663-2672.	3.0	30
58	Erosion rates across space and timescales from a multi-proxy study of rivers of eastern Taiwan. Global and Planetary Change, 2017, 157, 174-193.	3.5	30
59	Boundary scavenging at the East Atlantic margin does not negate use of 231Pa/230Th to trace Atlantic overturning. Earth and Planetary Science Letters, 2012, 333-334, 317-331.	4.4	29
60	10Be dating of Neogene halite. Geochimica Et Cosmochimica Acta, 2013, 122, 418-429.	3.9	29
61	Unravelling 5 decades of anthropogenic 236U discharge from nuclear reprocessing plants. Science of the Total Environment, 2020, 717, 137094.	8.0	29
62	Low energy AMS of americium and curium. Nuclear Instruments & Methods in Physics Research B, 2014, 331, 225-232.	1.4	28
63	Multiple advances of Alpine glaciers into the Jura Mountains in the Northwestern Switzerland. Swiss Journal of Geosciences, 2015, 108, 225-238.	1.2	28
64	Kinetically limited weathering at low denudation rates in semiarid climatic conditions. Journal of Geophysical Research F: Earth Surface, 2016, 121, 336-350.	2.8	28
65	Continuous 25-yr aerosol records at coastal Antarctica: Part 2: variability of the radionuclides ⁷ Be, ¹⁰ Be and ²¹⁰ Pb. Tellus, Series B: Chemical and Physical Meteorology, 2022, 63, 920.	1.6	27
66	Detection of UH3+ and ThH3+ molecules and 236U background studies with low-energy AMS. Nuclear Instruments & Methods in Physics Research B, 2013, 294, 364-368.	1.4	27
67	Evolution of soil erosion rates in alpine soils of the Central Rocky Mountains using fallout Pu and δ13C. Earth and Planetary Science Letters, 2018, 496, 257-269.	4.4	27
68	Accelerator mass spectrometry of 236U at low energies. Nuclear Instruments & Methods in Physics Research B, 2011, 269, 3199-3203.	1.4	26
69	Anthropogenic 236U and 129I in the Mediterranean Sea: First comprehensive distribution and constrain of their sources. Science of the Total Environment, 2017, 593-594, 745-759.	8.0	26
70	Anthropogenic ²³⁶ U in the North Sea – A Closer Look into a Source Region. Environmental Science & Technology, 2017, 51, 12146-12153.	10.0	26
71	Preliminary results of CoQtz-N: A quartz reference material for terrestrial in-situ cosmogenic 10Be and 26Al measurements. Nuclear Instruments & Methods in Physics Research B, 2019, 456, 203-212.	1.4	26
72	Protactinium-231: A new radionuclide for AMS. Nuclear Instruments & Methods in Physics Research B, 2007, 262, 379-384.	1.4	25

#	Article	IF	CITATIONS
73	Climatic and Tectonic forcing on alluvial fans in the Southern Central Andes. Quaternary Science Reviews, 2017, 172, 131-141.	3.0	25
74	Last glacial maximum glaciers in the Northern Apennines reflect primarily the influence of southerly storm-tracks in the western Mediterranean. Quaternary Science Reviews, 2018, 197, 352-367.	3.0	25
75	Tracing the temporal evolution of soil redistribution rates in an agricultural landscape using ²³⁹⁺²⁴⁰ Pu and ¹⁰ Be. Earth Surface Processes and Landforms, 2019, 44, 1783-1798.	2.5	25
76	Tracing Atlantic Waters Using ¹²⁹ I and ²³⁶ U in the Fram Strait in 2016. Journal of Geophysical Research: Oceans, 2019, 124, 882-896.	2.6	25
77	Postglacial erosion of bedrock surfaces and deglaciation timing: New insights from the Mont Blanc massif (western Alps). Geology, 2020, 48, 139-144.	4.4	25
78	Latest Pleistocene glacier advances and post-Younger Dryas rock glacier stabilization in the Mt. KrivÃjÅ^ group, High Tatra Mountains, Slovakia. Geomorphology, 2020, 358, 107093.	2.6	25
79	Highly resolved Beryllium-10 record from ODP Site 1089—A global signal?. Earth and Planetary Science Letters, 2007, 257, 245-258.	4.4	24
80	10Be in Ice Cores and 14C in Tree Rings: Separation of Production and Climate Effects. Space Science Reviews, 2013, 176, 343-349.	8.1	24
81	Measurement of 236U on the 1 MV AMS system at the Centro Nacional de Aceleradores (CNA). Nuclear Instruments & Methods in Physics Research B, 2015, 358, 45-51.	1.4	24
82	Accelerator Mass Spectrometry of 129I towards its lower limits. Nuclear Instruments & Methods in Physics Research B, 2015, 361, 445-449.	1.4	24
83	Timing of rockfalls in the Mont Blanc massif (Western Alps): evidence from surface exposure dating with cosmogenic 10Be. Landslides, 2018, 15, 1991-2000.	5.4	24
84	Cosmogenic radionuclides reveal an extreme solar particle storm near a solar minimum 9125 years BP. Nature Communications, 2022, 13, 214.	12.8	24
85	Sequential Injection Approach for Simultaneous Determination of Ultratrace Plutonium and Neptunium in Urine with Accelerator Mass Spectrometry. Analytical Chemistry, 2013, 85, 8826-8833.	6.5	23
86	Soil formation and weathering in a permafrost environment of the Swiss Alps: a multiâ€parameter and nonâ€steadyâ€state approach. Earth Surface Processes and Landforms, 2017, 42, 814-835.	2.5	23
87	Identifying slope processes over time and their imprint in soils of mediumâ€high mountains of Central Europe (the Karkonosze Mountains, Poland). Earth Surface Processes and Landforms, 2018, 43, 1195-1212.	2.5	23
88	Tracking rockglacier evolution in the Eastern Alps from the Lateglacial to the early Holocene. Quaternary Science Reviews, 2020, 241, 106424.	3.0	23
89	Relating the spatial variability of chemical weathering and erosion to geological and topographical zones. Geomorphology, 2020, 363, 107235.	2.6	23
90	The Ticino-Toce glacier system (Swiss-Italian Alps) in the framework of the Alpine Last Glacial Maximum. Quaternary Science Reviews, 2022, 279, 107400.	3.0	23

#	Article	IF	CITATIONS
91	Palaeoclimate, glacier and treeline reconstruction based on geomorphic evidences in the Mongun-Taiga massif (south-eastern Russian Altai) during the Late Pleistocene and Holocene. Quaternary International, 2018, 470, 26-37.	1.5	22
92	Tracing water masses with ¹²⁹ l and ²³⁶ U in the subpolar North Atlantic along the GEOTRACES GA01 section. Biogeosciences, 2018, 15, 5545-5564.	3.3	22
93	Quality assurance in accelerator mass spectrometry: Results from an international round-robin exercise for 10Be. Nuclear Instruments & Methods in Physics Research B, 2012, 289, 68-73.	1.4	21
94	10Be and 26Al low-energy AMS using He-stripping and background suppression via an absorber. Nuclear Instruments & Methods in Physics Research B, 2014, 331, 209-214.	1.4	21
95	Tectonic and lithological controls on denudation rates in the central Bolivian Andes. Tectonophysics, 2015, 657, 230-244.	2.2	21
96	Laser Ablation – Accelerator Mass Spectrometry: An Approach for Rapid Radiocarbon Analyses of Carbonate Archives at High Spatial Resolution. Analytical Chemistry, 2016, 88, 8570-8576.	6.5	21
97	Climate and reliefâ€induced controls on the temporal variability of denudation rates in a granitic upland. Earth Surface Processes and Landforms, 2019, 44, 2570-2586.	2.5	21
98	Proof-of-principle of a compact 300†kV multi-isotope AMS facility. Nuclear Instruments & Methods in Physics Research B, 2019, 439, 84-89.	1.4	21
99	Timing and flow pattern of the Orta Glacier (European Alps) during the Last Glacial Maximum. Boreas, 2020, 49, 315-332.	2.4	21
100	Tree-rings reveal two strong solar proton events in 7176 and 5259 BCE. Nature Communications, 2022, 13, 1196.	12.8	21
101	Landslide deposits as stratigraphical markers for a sequenceâ€based glacial stratigraphy: a case study of a Younger Dryas system in the Eastern Alps. Boreas, 2016, 45, 537-551.	2.4	20
102	Spatial and temporal variations in denudation rates derived from cosmogenic nuclides in four European fluvial terrace sequences. Geomorphology, 2016, 274, 180-192.	2.6	20
103	Long-term soil erosion derived from in-situ 10Be and inventories of meteoric 10Be in deeply weathered soils in southern Brazil. Chemical Geology, 2017, 466, 380-388.	3.3	20
104	Circulation timescales of Atlantic Water in the Arctic Ocean determined from anthropogenic radionuclides. Ocean Science, 2021, 17, 111-129.	3.4	20
105	Boron suppression with a gas ionization chamber at very low energies (E<1MeV). Nuclear Instruments & Methods in Physics Research B, 2010, 268, 843-846.	1.4	19
106	COSMOGENIC 21Ne AND 10Be REVEAL A MORE THAN 2 Ma ALLUVIAL FAN FLANKING THE CAPE MOUNTAINS, SOUTH AFRICA. South African Journal of Geology, 2015, 118, 129-144.	1.2	19
107	The competition between coastal trace metal fluxes and oceanic mixing from the ¹⁰ Be/ ⁹ Be ratio: Implications for sedimentary records. Geophysical Research Letters, 2017, 44, 8443-8452.	4.0	19
108	Lateglacial retreat chronology of the Scandinavian Ice Sheet in Finnmark, northern Norway, reconstructed from surface exposure dating of major end moraines. Quaternary Science Reviews, 2017, 177, 130-144.	3.0	19

#	Article	IF	CITATIONS
109	Late Cenozoic cooling history of the central Menderes Massif: Timing of the Büyük Menderes detachment and the relative contribution of normal faulting and erosion to rock exhumation. Tectonophysics, 2017, 717, 585-598.	2.2	19
110	Revised Quaternary glacial succession and post-LGM recession, southern Wind River Range, Wyoming, USA. Quaternary Science Reviews, 2018, 192, 167-184.	3.0	19
111	Timing of exotic, far-traveled boulder emplacement and paleo-outburst flooding in the central Himalayas. Earth Surface Dynamics, 2020, 8, 769-787.	2.4	19
112	In-phase millennial-scale glacier changes in the tropics and North Atlantic regions during the Holocene. Nature Communications, 2022, 13, 1419.	12.8	19
113	Determination of Atto- to Femtogram Levels of Americium and Curium Isotopes in Large-Volume Urine Samples by Compact Accelerator Mass Spectrometry. Analytical Chemistry, 2016, 88, 2832-2837.	6.5	18
114	Double response of glaciers in the Upper Peio Valley (Rhaetian Alps, Italy) to the Younger Dryas climatic deterioration. Boreas, 2017, 46, 783-798.	2.4	18
115	Spatio-temporal dynamics of sediment transfer systems in landslide-prone Alpine catchments. Solid Earth, 2019, 10, 1489-1503.	2.8	18
116	Muted multidecadal climate variability in central Europe during cold stadial periods. Nature Geoscience, 2021, 14, 651-658.	12.9	18
117	^{239,240} Pu and ²³⁶ U records of an ice core from the eastern Tien Shan (Central Asia). Journal of Glaciology, 2017, 63, 929-935.	2.2	17
118	Soil denudation rates in an oldâ€growth mountain temperate forest driven by tree uprooting dynamics, Central Europe. Land Degradation and Development, 2020, 31, 222-239.	3.9	17
119	Cosmogenic in situ 14C-10Be reveals abrupt Late Holocene soil loss in the Andean Altiplano. Nature Communications, 2021, 12, 2546.	12.8	17
120	Dynamics and legacy of 4.8 ka rock avalanche that dammed Zion Canyon, Utah, USA. GSA Today, 2016, 26, 4-9.	2.0	17
121	A simple conceptual model of abrupt glacial climate events. Nonlinear Processes in Geophysics, 2007, 14, 709-721.	1.3	16
122	The evolution of climatically driven weathering inputs into the western Arctic Ocean since the late Miocene: Radiogenic isotope evidence. Earth and Planetary Science Letters, 2015, 419, 111-124.	4.4	16
123	Environmental controls on ¹⁰ Beâ€based catchmentâ€everaged denudation rates along the western margin of the Peruvian Andes. Terra Nova, 2017, 29, 282-293.	2.1	16
124	Lateglacial and Early Holocene glacier stages - New dating evidence from the Meiental in central Switzerland. Geomorphology, 2019, 340, 15-31.	2.6	16
125	Glaciation's topographic control on Holocene erosion at the eastern edge of the Alps. Earth Surface Dynamics, 2016, 4, 895-909.	2.4	15
126	Late Pleistocene – Holocene surface processes and landscape evolution in the central Swiss Alps. Geomorphology, 2017, 295, 306-322.	2.6	15

#	Article	IF	CITATIONS
127	U–Th and ¹⁰ Be constraints on sediment recycling in proglacial settings, Lago Buenos Aires, Patagonia. Earth Surface Dynamics, 2018, 6, 121-140.	2.4	15
128	Distribution of 236U in the U.S. GEOTRACES Eastern Pacific Zonal Transect and its use as a water mass tracer. Chemical Geology, 2019, 517, 44-57.	3.3	15
129	Last Lateglacial glacier advance in the Gran Paradiso Group reveals relatively drier climatic conditions established in the Western Alps since at least the Younger Dryas. Quaternary Science Reviews, 2021, 255, 106815.	3.0	15
130	Drainage basin dynamics during the transition from early to mature orogeny in Southern Taiwan. Earth and Planetary Science Letters, 2021, 562, 116874.	4.4	15
131	Denudation rates of small transient catchments controlled by former glaciation: The Hörnli nunatak in the northeastern Swiss Alpine Foreland. Quaternary Geochronology, 2014, 19, 135-147.	1.4	14
132	Probing the Kinetic Parameters of Plutonium–Naturally Occurring Organic Matter Interactions in Freshwaters Using the Diffusive Gradients in Thin Films Technique. Environmental Science & Technology, 2016, 50, 5103-5110.	10.0	14
133	Millennial scale variability of denudation rates for the last 15 kyr inferred from the detrital ¹⁰ Be record of Lake Stappitz in the Hohe Tauern massif, Austrian Alps. Holocene, 2017, 27, 1914-1927.	1.7	14
134	10Be-inferred paleo-denudation rates imply that the mid-Miocene western central Andes eroded as slowly as today. Scientific Reports, 2018, 8, 2299.	3.3	14
135	10Be surface exposure dating of the last deglaciation in the Aare Valley, Switzerland. Swiss Journal of Geosciences, 2018, 111, 295-303.	1.2	14
136	Presence of 236U and 239,240Pu in soils from Southern Hemisphere. Journal of Environmental Radioactivity, 2018, 192, 478-484.	1.7	14
137	The impact of stormâ€triggered landslides on sediment dynamics and catchmentâ€wide denudation rates in the southern Central Range of Taiwan following the extreme rainfall event of Typhoon Morakot. Earth Surface Processes and Landforms, 2020, 45, 548-564.	2.5	14
138	¹⁰ Be/ ⁹ Be Ratios Reveal Marine Authigenic Clay Formation. Geophysical Research Letters, 2020, 47, e2019GL086061.	4.0	14
139	231Pa/230Th: A proxy for upwelling off the coast of West Africa. Nuclear Instruments & Methods in Physics Research B, 2010, 268, 1159-1162.	1.4	13
140	Beryllium isotopes as tracers of Lake Lisan (last Glacial Dead Sea) hydrology and the Laschamp geomagnetic excursion. Earth and Planetary Science Letters, 2014, 400, 233-242.	4.4	13
141	Constant denudation rates in a high alpine catchment for the last 6 kyrs. Earth Surface Processes and Landforms, 2017, 42, 1065-1077.	2.5	13
142	Holocene evolution of the Triftje- and the Oberseegletscher (Swiss Alps) constrained with 10Be exposure and radiocarbon dating. Swiss Journal of Geosciences, 2018, 111, 117-131.	1.2	13
143	Regional-scale abrupt Mid-Holocene ice sheet thinning in the western Ross Sea, Antarctica. Geology, 2021, 49, 278-282.	4.4	13
144	Deciphering the evolution of the Bleis Marscha rock glacier (Val d'Err, eastern Switzerland) with cosmogenic nuclide exposure dating, aerial image correlation, and finite element modeling. Cryosphere, 2021, 15, 2057-2081.	3.9	13

#	Article	IF	CITATIONS
145	Are Compact AMS Facilities a Competitive Alternative to Larger Tandem Accelerators?. Radiocarbon, 2010, 52, 319-330.	1.8	12
146	Cosmogenic 36Cl in karst waters from Bunker Cave North Western Germany – A tool to derive local evapotranspiration?. Geochimica Et Cosmochimica Acta, 2012, 86, 138-149.	3.9	12
147	10Be in lacustrine sediments—A record of solar activity?. Journal of Atmospheric and Solar-Terrestrial Physics, 2012, 80, 92-99.	1.6	12
148	Subglacial abrasion rates at Goldbergkees, Hohe Tauern, Austria, determined from cosmogenic ¹⁰ Be and ³⁶ Cl concentrations. Earth Surface Processes and Landforms, 2017, 42, 1119-1131.	2.5	12
149	Bayesian inversion of a CRN depth profile to infer Quaternary erosion of the northwestern Campine Plateau (NE Belgium). Earth Surface Dynamics, 2017, 5, 331-345.	2.4	12
150	Laser ablation–accelerator mass spectrometry reveals complete bomb 14C signal in an otolith with confirmation of 60-year longevity for red snapper (Lutjanus campechanus). Marine and Freshwater Research, 2019, 70, 1768.	1.3	12
151	Chemical Versus Mechanical Denudation in Metaâ€Clastic and Carbonate Bedrock Catchments on Crete, Greece, and Mechanisms for Steep and High Carbonate Topography. Journal of Geophysical Research F: Earth Surface, 2019, 124, 2943-2961.	2.8	12
152	Changes in landscape evolution patterns in the northern Swiss Alpine Foreland during the mid-Pleistocene revolution. Bulletin of the Geological Society of America, 2019, 131, 2056-2078.	3.3	12
153	Tracing erosion rates in loess landscape of the Trzebnica Hills (Poland) over time using fallout and cosmogenic nuclides. Journal of Soils and Sediments, 2021, 21, 2952.	3.0	12
154	On the measurement of 10Be on the 1MV compact AMS system at the Centro Nacional de Aceleradores (Spain). Nuclear Instruments & Methods in Physics Research B, 2010, 268, 733-735.	1.4	11
155	Correlation of fluvial terraces and temporal steady-state incision on the onshore Makran accretionary wedge in southeastern Iran: Insight from channel profiles and 10Be exposure dating of strath terraces. Bulletin of the Geological Society of America, 2015, 127, 560-583.	3.3	11
156	Exposure dating of a pronounced glacier advance at the onset of the late-Holocene in the central Tyrolean Alps. Holocene, 2017, 27, 1350-1358.	1.7	11
157	Continuous 25-yr aerosol records at coastal Antarctica Part 2: variability of the radionuclides ₇ Be, ₁₀ Be and ₂₁₀ Pb. Tellus, Series B: Chemical and Physical Meteorology, 2011, 63, .	1.6	11
158	The role of frost cracking in local denudation of steep Alpine rockwalls over millennia (Eiger,) Tj ETQq0 0 0 rgBT	/Overlock	10 Tf 50 222
159	Carrier-free measurements of natural 10Be/9Be ratios at low energies. Nuclear Instruments & Methods in Physics Research B, 2010, 268, 726-729.	1.4	10
160	Variations in the depositional fluxes of cosmogenic beryllium on short time scales. Atmospheric Environment, 2011, 45, 2836-2841.	4.1	10
161	Existence of triply charged actinide-hydride molecules. Physical Review A, 2012, 85, .	2.5	10
162	26Al measurements below 500 kV in charge state 2+. Nuclear Instruments & Methods in Physics	1.4	10

Research B, 2015, 361, 257-262.

#	Article	IF	CITATIONS
163	Simulating ice core ¹⁰ Be on the glacial–interglacial timescale. Climate of the Past, 2015, 11, 115-133.	3.4	10
164	Novel Laser Ablation Sampling Device for the Rapid Radiocarbon Analysis of Carbonate Samples by Accelerator Mass Spectrometry. Radiocarbon, 2016, 58, 419-435.	1.8	10
165	Effective separation of Am(III) and Cm(III) using a DGA resin via the selective oxidation of Am(III) to Am(V). Journal of Radioanalytical and Nuclear Chemistry, 2019, 321, 227-233.	1.5	10
166	The ¹⁰ Be deglaciation chronology of the Göschenertal, central Swiss Alps, and new insights into the Göschenen Cold Phases. Boreas, 2019, 48, 867-878.	2.4	10
167	Electron spin resonance (ESR), optically stimulated luminescence (OSL) and terrestrial cosmogenic radionuclide (TCN) dating of quartz from a Plio-Pleistocene sandy formation in the Campine area, NE Belgium. Quaternary International, 2020, 556, 144-158.	1.5	10
168	The Potential of ²³³ U/ ²³⁶ U as a Water Mass Tracer in the Arctic Ocean. Journal of Geophysical Research: Oceans, 2022, 127, .	2.6	10
169	Direct coupling of a laser ablation cell to an AMS. Nuclear Instruments & Methods in Physics Research B, 2013, 294, 287-290.	1.4	9
170	Carrier free 10Be/9Be measurements with low-energy AMS: Determination of sedimentation rates in the Arctic Ocean. Nuclear Instruments & Methods in Physics Research B, 2013, 294, 67-71.	1.4	9
171	Minor inheritance inhibits the calibration of the ¹⁰ Be production rate from the AD 1717 Val Ferret rock avalanche, European Alps. Journal of Quaternary Science, 2014, 29, 318-328.	2.1	9
172	Charge state distributions and charge exchange cross sections of carbon in helium at 30–258 keV. Nuclear Instruments & Methods in Physics Research B, 2015, 361, 541-547.	1.4	8
173	Preparation of a multi-isotope plutonium AMS standard and preliminary results of a first inter-lab comparison. Nuclear Instruments & Methods in Physics Research B, 2015, 361, 327-331.	1.4	8
174	Optimizing the analyte introduction for 14C laser ablation-AMS. Journal of Analytical Atomic Spectrometry, 2017, 32, 1813-1819.	3.0	8
175	Chronology of alluvial terrace sediment accumulation and incision in the Pativilca Valley, western Peruvian Andes. Geomorphology, 2018, 315, 45-56.	2.6	8
176	Differential erosion and sediment fluxes in the Landquart basin and possible relationships to lithology and tectonic controls. Swiss Journal of Geosciences, 2019, 112, 453-473.	1.2	8
177	Postglacial to Holocene landscape evolution and process rates in steep alpine catchments. Earth Surface Processes and Landforms, 2019, 44, 242-258.	2.5	8
178	Fluvial dynamics and ¹⁴ Câ€ ¹⁰ Be disequilibrium on the Bolivian Altiplano. Earth Surface Processes and Landforms, 2019, 44, 766-780.	2.5	8
179	Geodynamic importance of the strike-slip faults at the eastern part of the Anatolian Scholle: Inferences from the uplift and slip rate of the Malatya Fault (Malatya-Ovacık Fault Zone, eastern) Tj ETQq1 1 C).7824314 r	gB & /Overloc
180	Integrated multi-temporal analysis of the displacement behaviour and morphology of a deep-seated compound landslide (Cerentino, Switzerland). Engineering Geology, 2020, 270, 105577.	6.3	8

#	Article	IF	CITATIONS
181	236U, 237Np and 239,240Pu as complementary fingerprints of radioactiveeffluents in the western Mediterranean Sea and in the Canada Basin (Arctic Ocean). Science of the Total Environment, 2021, 765, 142741.	8.0	8
182	Glacial erosion by the Trift glacier (Switzerland): Deciphering the development of riegels, rock basins and gorges. Geomorphology, 2021, 375, 107533.	2.6	8
183	Retreat of the Great Escarpment of Madagascar From Geomorphic Analysis and Cosmogenic ¹⁰ Be Concentrations. Geochemistry, Geophysics, Geosystems, 2021, 22, e2021GC009979.	2.5	8
184	Mid-Holocene thinning of David Glacier, Antarctica: chronology and controls. Cryosphere, 2021, 15, 5447-5471.	3.9	8
185	41Ca, 14C and 10Be concentrations in coral sand from the Bikini atoll. Journal of Environmental Radioactivity, 2014, 129, 68-72.	1.7	7
186	Constraints on Water Reservoir Lifetimes From Catchmentâ€Wide ¹⁰ Be Erosion Rates—A Case Study From Western Turkey. Water Resources Research, 2017, 53, 9206-9224.	4.2	7
187	Development of a multi-method chronology spanning the Last Glacial Interval from Orakei maar lake, Auckland, New Zealand. Geochronology, 2020, 2, 367-410.	2.5	7
188	Authigenic Be as a tool to date river terrace sediments? – An example from a Late Miocene hominid locality in Bulgaria. Quaternary Geochronology, 2015, 29, 6-15.	1.4	6
189	Simulation of ion beam scattering in a gas stripper. Nuclear Instruments & Methods in Physics Research B, 2015, 361, 237-244.	1.4	6
190	ColPuS, a new multi-isotope plutonium standard for Accelerator Mass Spectrometry. Nuclear Instruments & Methods in Physics Research B, 2019, 438, 189-192.	1.4	6
191	A novel chronometry technique for dating irradiated uranium fuels using Cm isotopic ratios. Journal of Radioanalytical and Nuclear Chemistry, 2019, 322, 1611-1620.	1.5	6
192	Spatial patterns of erosion and landscape evolution in a bivergent metamorphic core complex revealed by cosmogenic 10Be: The central Menderes Massif (western Turkey). , 2019, 15, 1846-1868.		6
193	Shortâ€ŧime (<10 ka) denudation rates as a marker of active folding in the Zagros Fold Belt (Iran). Terra Nova, 2019, 31, 111-119.	2.1	6
194	Local and global trace plutonium contributions in fast breeder legacy soils. Nature Communications, 2021, 12, 1381.	12.8	6
195	The potential for a continuous 10Be record measured on ice chips from a borehole. Results in Geochemistry, 2021, 5, 100012.	0.8	6
196	Age of the Most Extensive Claciation in the Alps. Geosciences (Switzerland), 2022, 12, 39.	2.2	6
197	Direct search for primordial 244Pu in Bayan Obo bastnaesite. Chinese Chemical Letters, 2022, 33, 3522-3526.	9.0	6

Sensitivity and response of beryllium $\hat{a} \in 10$ in marine sediments to rapid production changes (geomagnetic) Tj ETQ $\hat{0}$ 0 rgB $\frac{1}{2}$ /Overlock

#	Article	IF	CITATIONS
199	New Be-cathode preparation method for the ETH 6MV Tandem. Nuclear Instruments & Methods in Physics Research B, 2013, 294, 199-202.	1.4	5
200	Speciation and Bioavailability Measurements of Environmental Plutonium Using Diffusion in Thin Films. Journal of Visualized Experiments, 2015, , e53188.	0.3	5
201	Glaciation history of Queen Maud Land (Antarctica) – New exposure data from nunataks. Nuclear Instruments & Methods in Physics Research B, 2015, 361, 599-603.	1.4	5
202	Evidence of plutonium bioavailability in pristine freshwaters of a karst system of the Swiss Jura Mountains. Geochimica Et Cosmochimica Acta, 2017, 206, 30-39.	3.9	5
203	Possible climatic controls on the accumulation of Peru's most prominent alluvial fan: The Lima Conglomerate. Earth Surface Processes and Landforms, 2019, 44, 991-1003.	2.5	5
204	Unravelling Quasi-Continuous 14C Profiles by Laser Ablation AMS. Radiocarbon, 2020, 62, 453-465.	1.8	5
205	Quaternary landscape evolution in the Western Argentine Precordillera constrained by 10Be cosmogenic dating. Geomorphology, 2022, 396, 107984.	2.6	5
206	Scavenged 239Pu, 240Pu, and 241Am from snowfalls in the atmosphere settling on Mt. Zugspitze in 2014, 2015 and 2016. Scientific Reports, 2017, 7, 11848.	3.3	4
207	Lagged atmospheric circulation response in the Black Sea region to Greenland Interstadial 10. Proceedings of the National Academy of Sciences of the United States of America, 2020, 117, 28649-28654.	7.1	4
208	Build-up and chronology of blue ice moraines in Queen Maud Land, Antarctica. Quaternary Science Advances, 2020, 2, 100012.	1.9	4
209	Impact of nuclear fuel reprocessing on the temporal evolution of marine radiocarbon. Science of the Total Environment, 2020, 738, 139700.	8.0	4
210	Ultrasensitive Analytical Method for Direct Search of Primordial 244Pu in Bastnaesite. ACS Earth and Space Chemistry, 2021, 5, 1316-1324.	2.7	4
211	Quaternary landscape evolution of patagonia at the Chilean Triple Junction: Climate and tectonic forcings. Quaternary Science Reviews, 2021, 261, 106960.	3.0	4
212	²³⁶ U/ ²³⁸ U Analysis of Femtograms of ²³⁶ U by MC-ICPMS. Analytical Chemistry, 2021, 93, 8442-8449.	6.5	4
213	Complex patterns of schist tor exposure and surface uplift, Otago (New Zealand). Geomorphology, 2021, 389, 107849.	2.6	4
214	Piecing together the Lateglacial advance phases of the Reussgletscher (central Swiss Alps). Geographica Helvetica, 2018, 73, 241-252.	0.8	4
215	Source to sink analysis of weathering fluxes in Lake Baikal and its watershed based on riverine fluxes, elemental lake budgets, REE patterns, and radiogenic (Nd, Sr) and 10Be/9Be isotopes. Geochimica Et Cosmochimica Acta, 2022, 321, 133-154.	3.9	4
216	Passive Sampling Tool for Actinides in Spent Nuclear Fuel Pools. ACS Omega, 2022, 7, 20053-20058.	3.5	4

#	Article	IF	CITATIONS
217	Rapid Revelation of Radiocarbon Records with Laser Ablation Accelerator Mass Spectrometry. Chimia, 2014, 68, 215.	0.6	3
218	¹⁰ Be depth profiles in glacial sediments on the Swiss Plateau: deposition age, denudation and (pseudo-) inheritance. E&G Quaternary Science Journal, 2017, 66, 57-68.	0.7	3
219	De-icing landsystem model for the Universidad Glacier (34° S) in the Central Andes of Chile during the past ~660Âyears. Geomorphology, 2022, 400, 108096.	2.6	3
220	Reconstructing the depositional history of Pleistocene fluvial deposits based on grain size, elemental geochemistry and in-situ 10Be data. Geomorphology, 2022, 402, 108127.	2.6	3
221	Contrasting soil dynamics in a formerly glaciated and non-glaciated Mediterranean mountain plateau (Serra da Estrela, Portugal). Catena, 2022, 215, 106314.	5.0	3
222	Bioavailable actinide fluxes to the Irish Sea from Sellafield-labelled sediments. Water Research, 2022, 221, 118838.	11.3	3
223	Evaluating debrisâ€flow and anthropogenic disturbance on ¹⁰ Be concentration in mountain drainage basins: implications for functional connectivity and denudation rates across time scales. Earth Surface Processes and Landforms, 2020, 45, 3955-3974.	2.5	2
224	Cosmogenic and Geological Evidence for the Occurrence of a Ma-Long Feedback between Uplift and Denudation, Chur Region, Swiss Alps. Geosciences (Switzerland), 2021, 11, 339.	2.2	2
225	10Be and 14C data provide insight on soil mass redistribution along gentle slopes and reveal ancient human impact. Journal of Soils and Sediments, 2021, 21, 3770-3788.	3.0	2
226	Initial tests of 26Al fluoride target matrix on MILEA AMS system. Nuclear Instruments & Methods in Physics Research B, 2021, 503, 45-52.	1.4	2
227	Calibrating a long-term meteoric ¹⁰ Be delivery rate into eroding western US glacial deposits by comparing meteoric and in situ produced ¹⁰ Be depth profiles. Geochronology, 2020, 2, 411-423.	2.5	2
228	A record of ²⁴¹ Am, ²³⁶ U, ²³⁸ U, ²³⁹ Pu, ²⁴⁰ Pu, ¹³⁴ Cs and ¹³⁷ Cs in surface seawater and ²⁴¹ Am in aerosols shortly after the FDNPP incident occurred. Geochemical Journal, 2021, 55, 33-38.	1.0	2
229	Further improvement for 10Be measurement on an upgraded compact AMS radiocarbon facility. Nuclear Instruments & Methods in Physics Research B, 2015, 361, 178-182.	1.4	1
230	A Comparison of \hat{I}^3 -ray Spectroscopy with Accelerator Mass Spectrometry for the Environmental Assay of Plutonium. , 2018, , .		1
231	10 Be surface exposure dating reveals unexpected high deformation rates in the central Andean wedge interior. Terra Nova, 2021, 33, 30-45.	2.1	1
232	Rapid post-glacial bedrock weathering in coastal Norway. Geomorphology, 2022, 397, 108003.	2.6	1
233	Reconsidering the origin of the Sedrun fans (Graubünden, Switzerland). E&G Quaternary Science Journal, 2018, 67, 17-23.	0.7	1
234	Early Pleistocene complex cut-and-fill sequences in the Alps. Swiss Journal of Geosciences, 2022, 115, .	1.2	1

#	Article	IF	CITATIONS
235	Spatio-temporal variability and controlling factors for postglacial denudation rates in the Dora Baltea catchment (western Italian Alps). Earth Surface Dynamics, 2022, 10, 493-512.	2.4	1
236	Landscape evolution, post-LGM surface denudation and soil weathering processes from Dickinson Park mire, Wind River Range, Wyoming (USA). Geomorphology, 2020, 371, 107433.	2.6	0
237	Transformation of high-relief canyon topography by an ancient rock avalanche, Hop Valley, Zion National Park, Utah, USA. Holocene, 2021, 31, 720-731.	1.7	0
238	Advance in the Mapping of the 1717 AD Triolet Rock Avalanche Deposit (Mont Blanc Massif, Italy) Using Cosmogenic Exposure Dating. , 2013, , 185-189.		0
239	ULTRA-TRACE DETERMINATION OF NEPTUNIUM-237 AND PLUTONIUM ISOTOPES IN URINE SAMPLES BY COMPACT ACCELERATOR MASS SPECTROMETRY. AECL Nuclear Review, 2015, 4, 125-130.	0.1	0
240	NEW ¹⁰ BE EXPOSURE AGES FOR PLEISTOCENE GLACIAL STRATIGRAPHY, SOUTHERN WIND RIVER RANGE, WYOMING, USA. , 2017, , .		0
241	Delayed Western Gotland Basin (Baltic Sea) ventilation in response to the onset of a Mid-Holocene climate oscillation. Quaternary Science Reviews, 2021, 273, 107253.	3.0	0